HHS Public Access

Author manuscript

Cell Rep. Author manuscript; available in PMC 2018 November 06.

Published in final edited form as:

Cell Rep. 2018 September 18; 24(12): 3224–3236. doi:10.1016/j.celrep.2018.08.058.

ΔNp63α Suppresses TGFB2 Expression and RHOA Activity to Drive Cell Proliferation in Squamous Cell Carcinomas

Christopher G. Abraham[1], **Michael P. Ludwig**[1], **Zdenek Andrysik**[1], **Ahwan Pandey**[1], **Molishree Joshi**[2], **Matthew D. Galbraith**[1], **Kelly D. Sullivan**[1,2,3], and **Joaquin M. Espinosa**[1,2,3,4,*]

[1]Department of Pharmacology, University of Colorado School of Medicine, Aurora, CO 80045, USA

[2]Functional Genomics Facility, University of Colorado School of Medicine, Aurora, CO 80045, USA

[3]Linda Crnic Institute for Down Syndrome, University of Colorado School of Medicine, Aurora, CO 80045, USA

[4]Department of Molecular, Cellular and Developmental Biology, University of Colorado Boulder, Boulder, CO 80203, USA

SUMMARY

The transcriptional repressor ΔNp63α is a potent oncogene widely overexpressed in squamous cell carcinomas (SCCs) of diverse tissue origins, where it promotes malignant cell proliferation and survival. We report here the results of a genome-wide CRISPR screen to identify pathways controlling ΔNp63α-de- pendent cell proliferation, which revealed that the small GTPase RHOA blocks cell division upon ΔNp63α knockdown. After ΔNp63α depletion, RHOA activity is increased, and cells undergo RHOA-depen- dent proliferation arrest along with transcriptome changes indicative of increased TGF-β signaling. Mechanistically, ΔNp63α represses transcription of *TGFB2,* which induces a cell cycle arrest that is partially dependent on RHOA. Ectopic TGFB2 activates RHOA and impairs SCC proliferation, and TGFB2 neutralization restores cell proliferation during ΔNp63α depletion. Genomic data from tumors demonstrate inactivation of RHOA and the TGFBR2 receptor and DNp63a overexpression in more than 80% of lung SCCs.

*Correspondence: joaquin.espinosa@ucdenver.edu.

[5]Lead Contact

AUTHOR CONTRIBUTIONS

C.G.A. and M.P.L. conceived and designed experiments and acquired, analyzed, and interpreted data. Z.A. designed experiments and acquired, analyzed, and interpreted data. A.P. analyzed sequencing and TCGA data. M.J. provided reagents and designed experiments. M.D.G., K.D.S., and J.M.E. conceived and designed experiments, analyzed and interpreted data, and drafted and revised the manuscript.

DECLARATION OF INTERESTS

The authors declare no competing interests.

SUPPLEMENTAL INFORMATION

Supplemental Information includes Supplemental Experimental Procedures, three figures, and two tables and can be found with this article online at https://doi.org/10.1016/j.celrep.2018.08.058.

DATA AND SOFTWARE AVAILABILITY

The accession number for the CRISPR screen and RNA-seq data reported in this paper is GEO: GSE111635.

These results reveal a signaling pathway controlling SCC proliferation that is potentially amenable to pharmacological intervention.

In Brief

Abraham et al. employ a genome-wide CRISPR screening strategy to characterize the mechanism of action of the ΔNp63α oncogene in SCC. ΔNp63α suppresses *TGFB2* expression and RHOA activity to drive SCC proliferation. TGFB2 is sufficient to impair SCC proliferation and necessary to enforce cell cycle arrest upon depletion of ΔNp63α.

Graphical Abstract

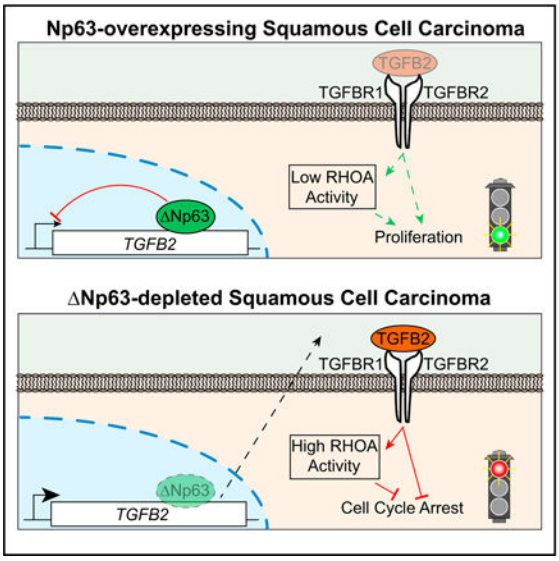

INTRODUCTION

The p63 isoform ΔNp63α is a member of the p53 family of transcription factors (García-Mariscal et al., 2018; Lawrence et al., 2014; Palomero et al., 2014; Rodrigues et al., 2014; Sa- kata-Yanagimoto et al., 2014). During development, ΔNp63α expression is restricted to epithelial stem cells and the undifferentiated basal layer of stratified epithelia, where it functions as an essential proliferative factor critical for epithelial maintenance and epidermal morphogenesis (Mills et al., 1999; Senoo et al., 2007; Yang et al., 1998). In fact, germline mutations in the *TP63* locus are associated with various ectodermal syndromes and developmental disorders (Brunner et al., 2002). In cancer, ΔNp63α functions as a potent oncogene in squamous cell carcinomas (SCCs) of diverse origins, where its overexpression is a marker of poor prognosis (Graziano and De Laurenzi, 2011). Although it is well established that ΔNp63α drives cell proliferation and blocks apoptosis in diverse cancer cell types, the precise mechanisms underlying these oncogenic properties are poorly characterized.

ΔNp63α harbors a DNA-binding domain similar to that found in the other p53 family members, and it binds to DNA sequences nearly identical to those bound by p53 and p73

(Perez et al., 2007). However, because ΔNp63α is transcribed from a downstream alternative promoter within the *TP63* locus, it lacks the N-terminal transcriptional activation domain found in the full- length forms of p53, p63, and p73. Accordingly, ΔNp63α is thought to act primarily as a transcriptional repressor (DeYoung et al., 2006; Mundt et al., 2010; Rocco et al., 2006; Westfall etal.,2003). Initially, it was hypothesized that DNp63a drives cancer progression by acting in a dominant-negative manner to repress p53 and/or p73 target genes involved in cell cycle arrest (e.g., *CDKN1A* and *SFN)* and apoptosis (e.g., *PMAIP1* and *BBC3)* (DeYoung et al., 2006; Rocco et al., 2006; Westfall et al., 2003; Yang et al., 1998). According to this model, DNp63a overexpression would inactivate the tumor-suppressive programs controlled by p53 and p73 by preventing access to their DNA binding sites. However, this model has been challenged by several observations. First, epidemiological studies demonstrated that most SCCs exhibit both overexpression of DNp63a and inactivating mutations in *TP53,* suggesting the existence of p53-independent oncogenic functions of DNp63a (Neil- sen et al., 2011; Nekulova et al., 2011). Second, in cancer cell types that co-express DNp63a and wild-type versions of p53 and p73, depletion of p53 or p73 does not rescue the proliferation arrest caused by ΔNp63α knockdown (Gallant-Behm and Espinosa, 2013; Gallant-Behm etal., 2012). In fact, the transcriptional programs controlled by DNp63a and p53 in these cell types are largely non-overlapping (Gallant-Behm et al., 2012). Third, ΔNp63α interacts with transcriptional repressor complexes, including the SRCAP histone exchange complex (Gallant-Behm et al., 2012) and HDAC1-HDAC2 lysine deacetylase complexes (LeBoeuf et al., 2010; Ramsey et al., 2011), which have been shown to be required for repression of specific subsets of ΔNp63α target genes in different cell types. Altogether, these observations reveal the existence of chromatin-based mechanisms of transcriptional repression by ΔNp63α acting independently of p53 and p73. Despite these advances, a key question remains unanswered: what are the keytumor-suppressive signaling pathways repressed by ΔNp63α during tumor progression?

To address this question, we performed a genome-wide CRISPR-based knockout screen in lung SCC cells that require expression of ΔNp63α to proliferate. We identified anti-proliferative genes whose knockout rescues the ability of these cells to proliferate when ΔNp63α is depleted as well as genes displaying synthetic lethality with ΔNp63α. Additionally, using RNA sequencing (RNA-seq) transcriptome profiling, we identified genes repressed by ΔNp63α. This combined approach revealed an anti-proliferative TGFB2/RHOA-centered signaling pathway that is suppressed by ΔNp63α to drive cell proliferation. Key aspects of this signaling pathway are conserved across SCC cell types, and its clinical relevance is supported by analyses of genomics data derived from hundreds of patient-derived tumor samples, which demonstrate downregulation of RHOA and TGFB2 receptors concurrent with DNp63a overexpression in ~80% of lung SCCs. Altogether, these results reveal a molecular mechanism by which ΔNp63α drives cancer progression.

RESULTS

A CRISPR Screen Identifies TGF-β and RHOA Signaling as Negative Regulators of ΔNp63α-Driven Cell Proliferation

Previous studies have demonstrated that ΔNp63α drives proliferation of SCCs of diverse origins (Graziano and De Laurenzi, 2011). To enable mechanistic investigations of ΔNp63α, we previously generated H226 lung SCC cells that stably express a doxycycline-inducible short hairpin RNA (shRNA) targeting all α and β p63 isoforms (denoted here as shp63) (Gallant-Behm et al., 2012). Importantly, ΔNp63α is the primary p63 isoform expressed in this cell line, which also expresses wild-type p53 and p73 (Gallant-Behm et al., 2012). Knockdown of ΔNp63α for 6 days in H226 cells blocks cell cycle progression, as seen by decreased cell numbers (Figure S1A) and reduced phospho- RB levels (Figure S1B), and this cell cycle arrest cannot be overcome by concomitant knockdown of p53 or p73 (Gallant-Behm and Espinosa, 2013; Gallant-Behm et al., 2012). Moreover, depletion of ΔNp63α does not induce apoptosis in this cell line, and the proliferation arrest is reversible upon restoration of ΔNp63α expression (i.e., removal of doxycycline) (Gallant- Behm et al., 2012).

To identify genes required for proliferation arrest upon ΔNp63α knockdown, we carried out a genetic loss-of-function screen (Figure 1A). Briefly, we transduced shp63-expressing H226 cells with two lentivirus-based CRISPR libraries (Shalem et al., 2014) consisting of ~119,000 single guide RNA (sgRNA) constructs targeting ~19,000 protein coding genes and 1,000 non-targeting control sgRNAs. After selection of cells carrying stably integrated sgRNAs, we included a propagation step to remove sgRNAs targeting essential genes. In duplicate, the resulting cell populations were treated for 14 days with vehicle (PBS) or doxycycline (to induce ΔNp63α knockdown). During this period of selection, we expected that cells containing sgRNAs targeting anti-proliferative genes acting during ΔNp63α depletion (referred to as p63-anti-proliferative genes [APGs]) would escape cell cycle arrest and continue to proliferate, whereas those with sgRNAs targeting synthetic lethal genes with DNp63a knockdown (p63-synthetic lethal genes [SLGs]) would drop out of the population, resulting in enrichment or depletion of those particular sgRNAs, respectively. At the end of the selection period, we harvested genomic DNA from the resulting cell populations and PCR-amplified sgRNA cassettes for quantification by next- generation sequencing and statistical analysis (see Experimental Procedures for more details).

Across all samples and both libraries, we detected 99% of sgRNAs. At the individual sgRNA level, differential expression from RNA-seq version 2 (DESeq2) analysis identified thousands of sgRNAs that were significantly enriched or depleted upon ΔNp63α knockdown (adjusted $p < 0.05$; Figure S1C; Table S1). To define high-confidence p63-APG and p63-SLG candidates at the gene level, we required at least two sgRNAs with significant changes of 2-fold or greater, resulting in 91 p63-APG and 50 p63-SLG candidates (Figure 1B; Table S1). Examples of observed fold changes for individual sgRNAs are shown in Figure 1C for *RHOA* (a candidate p63-APG), for which 4 of 6 sgRNAs were significantly enriched, and *ARHGAP35* (a candidate p63- SLG), for which 3 of 6 sgRNAs were significantly depleted. Importantly, of the 999 Non-targeting control sgRNAs we detected, only 51 displayed

significant changes of 2-fold or greater (Figure 1B; Table S1). In parallel, we performed a gene-level analysis using model-based analysis of genome-wide CRISPR- Cas9 knockout (MAGeCK) (Li et al., 2014), which scored 1,659 genes as candidate p63-APGs and 881 genes as candidate p63-SLGs ($p < 0.05$; Figure S1D; Table S1), including ~90% of our high-confidence candidates. Notably, fold change values for the top two sgRNAs for high-scoring genes in the MAGeCK analysis tend to have strong agreement (Figure S1E), supporting our minimum requirement of two sgRNAs per gene.

To gain insight into the potential functions of p63-APGs and p63-SLGs in SCCs, we interrogated our list of 141 high-confi- dence candidate genes for the presence of known signaling pathways using Ingenuity Pathway Analysis (Krämer et al., 2014). Many of the top-ranking enriched pathways ($p < 0.005$) share multiple p63-APG and p63-SLG candidate genes, among which the small GTPase RHOA is common to the largest number of pathways (9 of 16; Figure 1D). This analysis also revealed a clear involvement of transforming growth factor β (TGF-β) signaling because a large number of the pathways include TGFBR1, TGFBR2, and SMAD4 (Figure 1D). A number of additional hits in these top pathways encode products involved in RHOA signaling (Figure 1E), including known upstream activators of RHOA *(CSK, GNA12, ILK, TGFBR1,* and *TGFBR2)* (Khyrul et al., 2004; Nagao et al., 1999; Ottley and Gold, 2014), direct regulators of RHOA GTPase activity *(ARHGAP35* and *ARH- GEF12)* (Reuther et al., 2001; Zhang and Zheng, 1998), and known downstream effectors of RHOA signaling *(MYH9, PFN1,* and *VCL)* (Deakin et al., 2012; Moon et al., 2014; Watanabe et al., 1997). Of these p63-APG or SLG candidates, *RHOA, PFN1, SMAD4, TGFBR1,* and *TGFBR2* scored with three or four sgRNAs, further increasing our confidence in these hits (Figure 1F). Thus, our CRISPR screen identified RHOA and TGF-β signaling as potential modulators of ΔNp63α-dependent cell proliferation in SCCs. In particular, the involvement of RHOA caught our interest because RHOA is being increasingly recognized as a tumor suppressor frequently inactivated in diverse malignancies (García-Mariscal et al., 2018; Lawrence et al., 2014; Palomero et al., 2014; Rodrigues et al., 2014; Sakata-Yanagimoto et al., 2014), but its relationship to ΔNp63α-driven tumorigenesis has not been explored.

RHOA Signaling Blocks Cell Proliferation upon Depletion of ΔNp63α

To validate the effects of RHOA and TGF-β signaling on SCC proliferation, we performed transient, small interfering RNA (siRNA)-mediated knockdown of *RHOA, ARHGEF12, GNA12, ILK,* and *TGFBR2* alone and in combination with ΔNp63α knockdown in H226 cells (Figures S2A and S2B). As expected, depletion of ΔNp63α alone impaired cell cycle progression, as measured by the fraction of 5-ethynyl-2'-deoxyuridine (EdU)- positive nuclei at 72 hr (Figure 2A). All five candidates tested led to significant, albeit partial, rescue of the cell cycle arrest phenotype caused by depletion of ΔNp63α (Figure 2A). We also confirmed that *RHOA* knockdown rescued the proliferation defect caused by p63 knockdown in another SCC cell line, Cal27 (Figures S2C and S2D). Interestingly, this dependence on RHOA to sustain cell cycle arrest upon ΔNp63α depletion was not observed in the immortalized keratinocyte cell line HaCaT (Figures S2E and S2F), suggesting that this functional interaction may be unique to tumor cells.

Because our original hypothesis was that ΔNp63α drives SCC proliferation, at least in part, by suppressing anti-proliferative signaling pathways, we next examined the effect of DNp63a knockdown on expression of RHOA. Although ΔNp63α mRNA levels remained depleted over 6 days of knock-down, there was no significant effect on RHOA mRNA or protein levels over this time period (Figures 2B and 2C). We next tested whether knockdown of ΔNp63α affects the level of active RHOA. As a small GTPase, RHOA exists in both active (guanosine triphosphate [GTP]-bound) and inactive (guanosine diphosphate [GDP]-bound) forms. To quantify active RHOA, we employed a pull-down assay that relies on the affinity of the Rho-binding domain of Rhotekin, a well-characterized effector of this protein family, for the GTP-bound form of Rho proteins, followed by western blot detection using a RHOA-specific antibody (Figure 2C). This demonstrated that knockdown of ΔNp63α over 6 days leads to a statistically significant increase in active RHOA (Figure 2D). Depletion of ΔNp63α also led to an increase in active RHOA in Cal27 cells (Figure S2G). Furthermore, knockdown of ΔNp63α in H226 cells was associated with changes in actin distribution, as measured by phalloidin immunofluorescence (Figure 2E), consistent with the known role of RHOA in regulation of the cytoskeleton (Burridge and Wennerberg, 2004).

Finally, to determine whether an increase in active RHOA is sufficient to induce cell cycle arrest, we transfected H226 cells with expression constructs for wild-type (WT), constitutively active (G14V), and dominant-negative (T19N) RHOA (Nagao et al., 1999). Although both WT RHOA and the T19N mutant had a small positive effect on cell proliferation, only the constitutively active G14V mutant caused a significant decrease in cell proliferation 72 hr after transfection (Figure 2F). This effect was apparent despite lower expression of G14V relative to the WT and T19N RHOA proteins (Figure S2H).

Altogether, these results confirm that *RHOA* can act as a p63- APG, restraining SCC proliferation under conditions of low ΔNp63α expression, and demonstrate that RHOA activity is suppressed by ΔNp63α in two different SCC cell lines.

Components of the TGF-β and RHOA Signaling Networks Are Commonly Repressed in Lung SCC Tumors

We hypothesized that components of TGF-β and RHOA signaling identified by our CRISPR screen as p63-APGs might be dysregulated during SCC progression *in vivo*. To examine this, we analyzed data available from The Cancer Genome Atlas (TCGA) for lung SCC tumors (Cancer Genome Atlas Research Network, 2012). Consistent with its known role as an oncogene in SCC, *TP63* is amplified and/or overexpressed in more than 90% of these tumors (Figure 3A). In contrast, multiple components of the TGF-β and RHOA signaling networks aredownregu- lated in large fractions of these same tumors, including *TGFBR2, FERMT2, RHOA, ILK,* and *ARHGEF12* (Figure 3A). Compared with all 141 screen hits, *TP63* ranks as one of the most overexpressed genes in SCC tumors relative to normal lung tissue, whereas components of the TGF-β and RHOA signaling modules are among the most downregulated (Figure 3B). Furthermore, when ranked by their correlations with *TP63* expression, it is evident that several components, including *ILK, FERMT2, RHOA,* and *TGFBR2,* show strong anti-correlation with *TP63* expression (Figure 3C). Finally, although overexpression and/or gain of *TP63* is not prevalent in lung adenocarcinoma (AD),

downregulation and/or loss of *RHOA* is widespread in this context (Cancer Genome Atlas Research Network, 2014; Figure 3D), raising the possibility that suppression of RHOA might be important for tumor progression beyond SCC, a notion supported by the significant rate of RHOA inactivating mutations found in a pan-cancer analysis of 4752 human cancers representing 21 tumor types (Lawrence et al., 2014).

These observations indicate that several components of TGF-β and RHOA signaling, including RHOA itself as well as upstream regulators and downstream effectors, are commonly downregulated in SCC tumors that exhibit overexpression and/or gain of *TP63.* This suggests that these genes may indeed act in anti-proliferative pathways and, therefore, be downregulated during development of lung SCCs, particularly those driven by ΔNp63α.

ΔNp63α Represses Expression of TGFB2, an Upstream Activator of RHOA

We next sought to gain insight into potential mechanisms by which ΔNp63α might suppress the activity of RHOA and other p63-APGs to drive proliferation of SCC cells. Toward this end, we examined the effect of ΔNp63α depletion on the transcrip- tome by comparison of poly(A)-enriched RNA from shControl and shp63 H226 cells after 6 days of knockdown. Differential expression analysis using DESeq2 (Love et al., 2014) revealed widespread effects on the transcriptome, with thousands of transcripts significantly upregulated and downregulated (adjusted $p < 0.1$; Figure S3A; Table S2). Ingenuity Pathway Analysis identified a number of significantly enriched pathways among the differentially expressed genes ($p < 0.1$; Figures 4A and 4B). As expected given the cell cycle arrest phenotype elicited by ΔNp63α depletion, cell cycle regulation was highly enriched among the downregulated genes, as was RhoGDI signaling, which could negatively regulate RHOA activity (Kim et al., 2018). Conversely, Rho family signaling and ILK signaling were enriched among the upregulated genes, consistent with altered activity of RHOA signaling during knockdown of ΔNp63α. Notably, the TGF-β pathway was also positively enriched, within which both TGBFR2, itself a p63-APG, and its ligand TGFB2, are upregulated upon ΔNp63α knockdown. Gene set enrichment analysis (Subramanian et al., 2005) also detected negative enrichment of hallmark cell cycle-related genes (G2M checkpoint) and positive enrichment of TGF-β pathway genes (Figures 4C and 4D).

To identify genes consistently deregulated by ΔNp63α depletion regardless of cell type, we used a stringent threshold (adjusted p value < 0.1, $\log_2$ fold change > 0.4 or < −0.4) to compare our RNA-seq data with published microarray datasets from the FaDu head and neck SCC (HNSCC), JHU029 HNSCC, and HaCaT immortalized keratinocyte cell lines (Saladi et al., 2017). This revealed a large degree of cell type specificity, with only 22 genes common among the four datasets (Figure 4E). Remarkably, in addition to p63 itself, this core group included *TGFB2* and its receptor, *TGFBR2.* Of these core genes, only TGFBR2 scored in our genetic screen as a high-confidence APG (Figures 1D, 1E, 4E, S1D, and S3B). Therefore, we decided to investigate further the role of the TGFB2 signaling pathway in the cell cycle arrest phenotype observed upon ΔNp63α knockdown.

Analysis of mRNA levels by qRT-PCR confirmed that both *TGFB2* and *TGFBR2,* but not *TGFB1* and *TGFBR1,* are significantly upregulated at the mRNA level after 6 days of ΔNp63α knockdown (Figure 4F). Increased expression of TGFB2 was also evident at the

level of secreted TGFB2 protein, as measured by ELISA (Figure 4G), concurrent with activation of TGF-β signaling, as indicated by increased phosphorylation of TGFBR2 and SMAD2/3 (Figure 4H). Depletion of ΔNp63α also led to increased levels of *TGFB2* mRNA and secreted protein in Cal27 cells (Figures S3C and S3D). Consistent with a widespread role for ΔNp63α in repression of *TGFB2,* Pearson correlation analysis of the TCGA lung SCC expression data revealed a significant anti correlation between *TP63* and *TGFB2* mRNA levels (Figure S3E).

To investigate whether TGFB2 might be *directly* repressed at the transcriptional level by ΔNp63α, we first used Pattern Locator to identify p63 binding motifs at the *TGFB2* locus (Mrazek and Xie, 2006). We next examined chromatin immunoprecipitation sequencing (ChIP-seq) data for p63 from primary human keratinocytes (Kouwenhoven et al., 2010) and human normal foreskin (HNFK) cells (McDade et al, 2014) and identified several peaks of p63 enrichment at this locus (Figure 4I). An intragenic peak ~52 kb from the transcription start site coincides with a motif that is highly similar to the consensus p63 binding site when compared using Tomtom (p = 1.16E-04) (Gupta et al., 2007). To determine whether ΔNp63α binds at this location in H226 cells, we performed ChIP analysis of the *TGFB2* locus with a pan-p63 antibody (4A4) (Figure 4J). Our ChIP analysis indicates that DNp63a binding is highly enriched at this intragenic site and that knockdown of ΔNp63α largely abrogates this signal, reducing it to levels equivalent to the control immunoglobulin G (IgG) (Figure 4I). Although this does not strictly exclude the possibility of *indirect* repression, this newly defined p63 binding site at the *TGFB2* locus displays a similar level of enrichment above background as two known p63 target genes, SAMD9L and ZHX2 (Gallant-Behm et al., 2012; Figure S3F). Transcriptionally active, elongating RNA polymerase II is associated with phosphorylation of serine-2 within the heptad repeats of the C-terminal domain of the RPB1 subunit (RNA polymerase II [Pol II] S2P) (Zaborowska et al., 2016). Importantly, depletion of ΔNp63α correlates with *increased* levels of Pol II S2P throughout the *TGFB2* gene body, consistent with direct repression of transcription by ΔNp63α at this locus (Figure 4J).

Altogether, these results demonstrate that TGFB2 is a conserved target of ΔNp63α - mediated transcriptional repression.

Elevated TGFB2 Contributes to Cell Cycle Arrest upon Depletion of ΔNp63α

Having demonstrated that *TGFB2* expression is downregu- lated by ΔNp63α, we next examined the functional consequences of altered TGFB2 levels on SCC proliferation and RHOA signaling. First, we tested the effect of TGFB2 administration on the proliferative capacity of H226 cells, both the parental cell line and a derivative where RHOA was knocked out via CRISPR-mediated gene editing *(RHOA*$^{--}$; Figure 5A). We observed a dose-dependent reduction in cell number 72 hr after TGFB2 addition to the cell culture medium (Figure 5B).

Interestingly, although RHOA is required for maximal effect at higher concentrations of the ligand, TGFB2 retains anti-proliferative capacity in *RHOA*$^{--}$ cells (Figure 5B), consistent with RHOA being one of several recognized downstream effectors of TGFB signaling (Sanchez and Barnett, 2012). We also found that TGFB2 treatment increases the amount of

active RHOA after 72 hr (Figure 5C). Notably, the anti-proliferative effects of TGFB2 are also evident in Cal27 SCC cells and HaCaT immortalized keratinocytes after 72 hr of treatment (Figures 5D and 5E).

Finally, we hypothesized that, if DNp63a-mediated repression of *TGFB2* is critical for proliferation of H226 cells, then blockade of extracellular TGFB2 would rescue the cell cycle arrest caused by ΔNp63α knockdown. Indeed, neutralization with the TFGB1-, TFGB2-, and TFGB3-blocking antibody (1D11) for 4 days did rescue the defect in proliferation caused by ΔNp63α depletion (Figure 5F).

Taken together, these results support a model whereby ΔNp63α dampens TGF-β signaling through direct repression of *TGFB2,* in turn leading to depletion of active RHOA, to promote cell proliferation in SCC (Figure 5G).

DISCUSSION

Lung cancer is the leading cause of cancer-associated deaths in the United States and worldwide because of high incidence and poor survival rates, with non-small-cell lung cancer (NSCLC) comprising the majority of cases. Within NSCLC, in 2017 alone, SCCs were estimated to account for ~68,000 (or ~30%) of new cases in the United States and, because of a lack of effective targeted therapies, ~48,000 individuals succumbing to the disease. Therefore, there is an urgent need for the identification and validation of new therapeutic targets in lung SCC. Despite genetic heterogeneity among SCCs, clinical observations indicate that high ΔNp63α expression correlates with more aggressive, treatment-refractory tumors. Here we report the results of a genome-wide CRISPR screen aimed at identifying genes that mediate addiction to ΔNp63α, leading to the discovery that an antiproliferative TGFB2 to RHOA signaling pathway is suppressed by ΔNp63α through transcriptional repression of TGFB2.

The Rho GTPases are a family of 20 small G proteins with roles in regulating the cytoskeleton, cell polarity, cell migration, and the cell cycle (Karlsson et al., 2009). Depending on the context, RHOA has been characterized as a tumor promoter (Karlsson et al., 2009; Ridley, 2013) or tumor suppressor (Palomero et al., 2014; Rodrigues et al., 2014; Sakata-Yanagimoto et al., 2014; Yoo et al., 2014). Inactivating mutations in the effector binding domain have been identified in several cancer types, including HNSCC (Kakiuchi et al., 2014; Lawrence et al., 2014). Most recently, loss of *RHOA* was found to enhance tumor formation in a mouse model of skin cancer, where keratinocyte-specific deletion of *RHOA* led to faster-growing, less differentiated tumors and increased invasiveness (García-Mariscal et al., 2018). Thus, the role of RHOA in cancer appears to be context-specific, and the exact mechanisms by which RHOA exerts these effects remain to be deciphered. Analysis of TCGA data indicates that downregulation of *RHOA* is a common feature of lung SCCs (Figure 3A), and our experimental data demonstrate that ΔNp63α constrains RHOA activity (Figure 2D). Taken together, these observations suggest that RHOA has a tumor-suppressive role in lung SCCs.

Canonically, the three TGF-β ligands signal through their cognate receptors, *TGFBR1* and *TGFBR2,* to activate the SMAD family of transcription factors that coordinate a vast gene expression network (Massague, 2008, 2012). TGF-β signaling, although cell type-specific, is generally tumor- suppressive in healthy cells, promoting cytostasis and enforcing differentiation (Massague, 2008). This is consistent with downre- gulation of *TGFBR2* expression in nearly all lung SCCs (Figure 3A). Ourdata support a tumor-suppressive role for TGF-β signaling in SCC in several ways: *TGFBR1* and *TGFBR2* act as anti-proliferative factors upon ΔNp63α depletion (Figures 1D-1F), *TGFB2* is repressed by ΔNp63α (Figure 4), and TGFB2 is both necessary (Figure 5F) and sufficient (Figure 5B) to promote cell cycle arrest in H226 cells. In contrast to its tumor-suppressive role in healthy cells, TGF-β signaling promotes metastasis later in tumor progression by stimulating motility, epithelial-to-mesenchymal transition (EMT), and extravasation (Massague, 2012). This observation is particularly interesting because EMT is associated with cell cycle arrest (Mejlvang et al., 2007; Vega etal., 2004) and could thus contribute to the anti-proliferative functions of the TGFB2 to RHOA signaling pathway identified here. Further studies will be required todissectwhetherand howthefunctional interplay described here between ΔNp63α, TGFB2, and RHOA signaling changes at different stages of cancer development as well as during development of stratified epithelia.

Several recent studies have identified individual genes and pathways crucial for ΔNp63α -dependent SCC proliferation both *in vitro* and *in vivo* (Gallant-Behm et al., 2012; Huang et al., 2013; Ramsey et al., 2013; Saladi et al., 2017). The results described here identify repression of *TGFB2* and subsequent downregulation of RHOA activity as important mechanisms by which DNp63a drives unrestrained SCC proliferation (Figure 5G), thus significantly advancing our mechanistic understanding of this potent oncogene.

EXPERIMENTAL PROCEDURES Cell Culture and Proliferation Assays

H226 cells were cultured in RPMI 1640 medium (Thermo Fisher Scientific). Cal27, HaCaT, and HEK293FT cells were cultured in DMEM (Thermo Fisher Scientific). All media were supplemented with 10% fetal bovine serum (Peak Serum) and antibiotic and antimycotic (Anti-Anti, Thermo Fisher Scientific). Cellswere maintained at 37^0C in a humidified atmospherewith 5% CO2. Generation of H226 cell lines expressing doxycycline-inducible control and p63- targeting shRNAs was described previously (Gallant-Behm et al., 2012).

For siRNA-based knockdown experiments, actively proliferating cells synthesizing DNA were quantified using a Click-iT EdU Alexa Fluor 488 high content screening (HCS) assay (Thermo Fisher Scientific) according to the manufacturer's directions, with 2 hr10 μM EdU labeling and permeabilization with 0.25% Triton X-100. ImageJ (Schneider et al., 2012) was used to count fluorescein isothiocyanate (FITC)-positive and DAPI-stained cells.

Western Blotting—Sample preparation, quantitation, and western blotting were carried out as described previously (Gallant-Behm etal., 2012). Detectionwas bychemilumi-nescence using SuperSignal West Pico PLUS (Thermo Fisher Scientific), and images were captured with an ImageQuant LAS4000 digital camera system (GE Healthcare). The antibodies used are described in the Supplemental Experimental Procedures.

CRISPR Screen and Sequencing Library Preparation—Human GecKOv2 library lentiviral pool production, transduction ofH226shp63 cells, screening conditions, and preparation of Illumina sequencing libraries are described in the Supplemental Experimental Procedures.

CRISPR Screen Data Analysis—Data quality assessment, filtering, and mapping are described in the Supplemental Experimental Procedures. Statistical analysis of screen data at the individual sgRNA level was carried out with DESeq2 (Love et al., 2014) and at the gene level with MAGeCK (Li et al., 2014).

Validation of Candidate Genes by siRNA Knockdown—Cellswereseeded into 96-well or6-well plates(4,000 or100,000 cells perwell) and cultured overnight. The next day, the growth medium was replaced and allowed to equilibrate under standard culture conditions as above. Stealth siRNA Lipofectamine RNAiMAX (Thermo Fisher Scientific) complexes were prepared in OptiMEM (Thermo Fisher Scientific), with a final concentration of 10 nM each siRNA, and added to each well. The growth medium was replaced again 24 hr later, and cells were cultured for a further 72 hr, followed by the Click-iT EdU assay or harvesting of RNA for qRT-PCR. The sequences and catalog numbers for the siRNAs (Stealth RNAi, Thermo Fisher Scientific) are listed in the Supplemental Experimental Procedures.

Active RHOA Pull-Down Assay—For measurement of active RHOA following ΔNp63α knockdown, H226 shControl and shp63 cells or Cal27 cells (1.5×10^6) were seeded into 15-cm plates in complete medium supplemented with 1 μg/mL doxycycline and cultured for 4 days with daily replacement of medium containing 1 μg/mL doxycycline. Cells were then split 1:6 into 15-cm plates and cultured for a further 2 days. After 6 days of treatment, cells were harvested, and protein lysates were immediately subjected to a RHOA pull-down activation assay (Cytoskeleton) according to the manufacturer's directions.

For measurement of active RHOA following TGFB2 treatment, H226 or Cal27 cells (1.5×10^6) were seeded into two 15-cm plates of complete medium. After overnight incubation, the medium was replaced with serum-free medium to reduce the level of growth factor-stimulated active RHOA, followed by incubation for 72 hr. Cells were treated for 10 min with serum-free medium containing human recombinant TGFB2 ligand at 5 ng/mL (R&D Systems, 302- B2-002). Protein lysates were immediately assayed with the RHOA pull-down assay kit.

Immunofluorescence Imaging—H226 shControl and shp63 cells (1×10^5 perwell)werestained with Phalloidin- iFluor 488 (Abcam) and DAPI solution, imaged using an Olympus FV1000 confocal laser-scanning microscope, assembled into *z* stacks, and processed using ImageJ. Full details are provided in the Supplemental Experimental Procedures.

Expression of WT, G14V, and T19N RHOA—A cDNA clone with the *RHOA* open reading frame in the pLX304-Blast-V5 expression vector was obtained from the Center for Cancer Systems Biology (CCSB)-Broad Human ORFeome collection (clone ID 304_00100) maintained by the University of Colorado Anschutz Medical Campus Functional Genomics

Facility. Constitutively active and dominant-negative mutants were created using site-directed mutagenesis with the QuikChange Lightning site-directed mutagenesis kit (Agilent Technologies). Cells were transfected with each construct for 72 hr prior to counting. Full details are provided in the Supplemental Experimental Procedures.

Analysis of TCGA Data—Copy number variation (CNV) analysis was performed by using GISTIC 2.0.22 with the default setting (Mermel et al., 2011). Segmentation data were downloaded from TCGA (2016_01_28) using firehose_get v 0.4.5 (https://confluence.broadinstitute.org/display/GDAC/Download). Only data from samples published by Lawrence et al. (2014) were used for CNV analysis. Expression analysis was performed using RNA-seq by expectation maximization (RSEM) V2 values. Oncoprints were created using the ComplexHeatmap package in R. Heatmaps were created using the ggplot2 package in R.

RNA-Seq and qRT-PCR—Total RNA was extracted from cell pellets using TRI reagent (Sigma-Aldrich) or a PureLink RNA mini kit (Thermo Fisher Scientific) according to the manufacturer's directions. RNA-seq library preparation and sequencing and cDNA synthesis and qRT-PCR analysis are described in the Supplemental Experimental Procedures.

RNA-Seq Data Analysis—Data quality assessment, filtering, and mapping were carried out as described previously (Sullivan et al., 2016). Differential expression analysis was carried out using DESeq2 (Love et al., 2014). Full details are provided in the Supplemental Experimental Procedures.

TGFB2 ELISA—Secreted TGFB2 was quantified by sandwich ELISA (Raybiotech) according to the manufacturer's instructions after 6 days of p63 knockdown. Sample concentration values were determined by comparison with a purified TGFB2 standard curve. Full detailsare provided intheSupplemental Experimental Procedures.

ChIP Analysis—ChIP analysis of the *TGFB2* locus was carried out as described previously (Gallant-Behm et al., 2012). qPCR was carried out on ChIP-enriched DNA against a standard curve of input DNA, with amplicons tiling across the locus, using SYBR Select Master Mix for CFX (Thermo Fisher Scientific) on a Viia7 real-time PCR system (Thermo Fisher Scientific). Enrichment values for each amplicon were calculated as a percentage of the amplicon with maximum signal for each antibody. The antibodies and primers used for ChIP-qPCR are described in the Supplemental Experimental Procedures.

TGFβ2 Treatment—H226, Cal27, and HaCaT cells were plated at 50,000 per well in 6-well plates and incubated overnight in complete medium. The next day, thiswas replaced with complete medium containing human recombinant TGFB2 (R&D Systems), prepared by a 2-fold dilution series from 8 ng/mL to 0.0625 ng/mL, and replaced every 24 hr with fresh TGFB2. After 72 hr treatment, cells were trypsi- nized and counted.

TGFβ Neutralization Assay—H226 cells were plated at 50,000 per well in 6-well plates in triplicate in complete medium supplemented with 1 μg/mL doxycycline. TGFβ neutralizing antibody (1D11, Thermo Fisher Scientific, MA5-23795) was added to each at a

final concentration of 2 μg/mL and replenished at 24 and 72 hr. After 4-day incubation, cells were trypsinized and counted.

Statistical Analysis—Statistical analyses were performed using Microsoft Excel and GraphPad Prism. Two-sided unpaired Student's t tests were used to assess statistical significance at a level of $p < 0.05$. All data presented are a minimum of three replicates, and error bars represent SEM.

Supplementary Material

Refer to Web version on PubMed Central for supplementary material.

ACKNOWLEDGMENTS

This work was supported primarily by NIH grant R01CA117907 (to J.M.E.), an American Cancer Society post-doctoral fellowship (to C.G.A.), pilot funding from the University of Colorado Cancer Center (UCCC) Head and Neck Cancer Program and grant P30CA046934 supporting the UCCC's Functional Genomics Shared Resource.

REFERENCES

Brunner HG, Hamel BC, and Bokhoven Hv Hv. (2002). P63 gene mutations and human developmental syndromes. Am. J. Med. Genet. 112, 284–290. [PubMed: 12357472]

Burridge K, and Wennerberg K (2004). Rho and Rac take center stage. Cell 116, 167–179. [PubMed: 14744429]

Cancer Genome Atlas Research Network (2012). Comprehensive genomic characterization of squamous cell lung cancers. Nature 489, 519–525. [PubMed: 22960745]

Cancer Genome Atlas Research Network (2014). Comprehensive molecular profiling of lung adenocarcinoma. Nature 511, 543–550. [PubMed: 25079552]

Deakin NO, Ballestrem C, and Turner CE (2012). Paxillin and Hic-5 interaction with vinculin is differentially regulated by Rac1 and RhoA. PLoS ONE 7, e37990. [PubMed: 22629471]

DeYoung MP, Johannessen CM, Leong C-O, Faquin W, Rocco JW, and Ellisen LW (2006). Tumor-specific p73 up-regulation mediates p63 dependence in squamous cell carcinoma. Cancer Res. 66, 9362–9368. [PubMed: 17018588]

Gallant-Behm CL, and Espinosa JM (2013). DNp63a utilizes multiple mechanisms to repress transcription in squamous cell carcinoma cells. Cell Cycle 12, 409–416. [PubMed: 23324337]

Gallant-Behm CL, Ramsey MR, Bensard CL, Nojek I, Tran J, Liu M, Ellisen LW, and Espinosa JM (2012). ΔNp63α represses anti-proliferative genes via H2A.Z deposition. Genes Dev. 26, 2325–2336. [PubMed: 23019126]

García-Mariscal A, Li H, Pedersen E, Peyrollier K, Ryan KM, Stanley A, Quondamatteo F, and Brakebusch C (2018). LossofRhoApromotes skintu- mor formation and invasion by upregulation of RhoB. Oncogene 37, 847–860. [PubMed: 29059167]

Graziano V, and De Laurenzi V (2011). Role of p63 in cancer development. Biochem. Biophys. Acta 1816, 57–66. [PubMed: 21515338]

Gupta S, Stamatoyannopoulos JA, Bailey TL, and Noble WS (2007). Quantifying similarity between motifs. Genome Biol. 8, R24. [PubMed: 17324271]

Huang Y, Kesselman D, Kizub D, Guerrero-Preston R, and Ratovitski EA (2013). Phospho- ΔNp63α / microRNA feedback regulation in squamous carcinoma cells upon cisplatin exposure. Cell Cycle 12, 684–697. [PubMed: 23343772]

Kakiuchi M, Nishizawa T, Ueda H, Gotoh K, Tanaka A, Hayashi A, Yamamoto S, Tatsuno K, Katoh H, Watanabe Y, et al. (2014). Recurrent gain-of-function mutations of RHOA in diffuse-type gastric carcinoma. Nat. Genet. 46, 583–587. [PubMed: 24816255]

Karlsson R, Pedersen ED, Wang Z, and Brakebusch C (2009). Rho GTPase function in tumorigenesis. Biochim. Biophys. Acta 1796, 91–98. [PubMed: 19327386]

Khyrul WA, LaLonde DP, Brown MC, Levinson H, and Turner CE (2004). The integrin-linked kinase regulates cell morphology and motility in a rho-associated kinase-dependent manner. J. Biol. Chem. 279, 54131–54139. [PubMed: 15485819]

Kim JG, Islam R, Cho JY, Jeong H, Cap KC, Park Y, Hossain AJ, and Park JB (2018). Regulation of RhoA GTPase and various transcription factors in the RhoA pathway. J. Cell. Physiol. 233, 6381–6392. [PubMed: 29377108]

Kouwenhoven EN, van Heeringen SJ, Tena JJ, Oti M, Dutilh BE, Alonso ME, de la Calle-Mustienes E, Smeenk L, Rinne T, Parsaulian L, et al. (2010). Genome-wide profiling of p63 DNA-binding sites identifies an element that regulates gene expression during limb development in the 7q21 SHFM1 locus. PLoS Genet. 6, e1001065. [PubMed: 20808887]

Krämer A, Green J, Pollard J, Jr., and Tugendreich S (2014). Causal analysis approaches in Ingenuity Pathway Analysis. Bioinformatics 30, 523–530. [PubMed: 24336805]

Lawrence MS, Stojanov P, Mermel CH, Robinson JT, Garraway LA, Golub TR, Meyerson M, Gabriel SB, Lander ES, and Getz G (2014). Discovery and saturation analysis of cancer genes across 21 tumour types. Nature 505, 495–501. [PubMed: 24390350]

LeBoeuf M, Terrell A, Trivedi S, Sinha S, Epstein JA, Olson EN, Morrisey EE, and Millar SE (2010). Hdac1 and Hdac2 act redundantly to control p63 and p53 functions in epidermal progenitor cells. Dev. Cell 19, 807–818. [PubMed: 21093383]

Li W, Xu H, Xiao T, Cong L, Love MI, Zhang F, Irizarry RA, Liu JS, Brown M, and Liu XS (2014). MAGeCK enables robust identification of essential genes from genome-scale CRISPR/Cas9 knockout screens. Genome Biol. 15, 554. [PubMed: 25476604]

Love MI, Huber W, and Anders S (2014). Moderated estimation of fold change and dispersion for RNA-seq datawith DESeq2. Genome Biol. 15, 550. [PubMed: 25516281]

Massagué J (2008). TGFbeta in Cancer. Cell 134, 215–230. [PubMed: 18662538]

Massagué J (2012). TGFβ signalling in context. Nat. Rev. Mol. Cell Biol. 13, 616–630. [PubMed: 22992590]

Mathelier A, Fornes O, Arenillas DJ, Chen CY, Denay G, Lee J, Shi W, Shyr C, Tan G, Worsley-Hunt R, et al. (2016). JASPAR 2016: a major expansion and update of the open-access database of transcription factor binding profiles. Nucleic Acids Res. 44 (D1), D110–D115. [PubMed: 26531826]

McDade SS, Patel D, Moran M, Campbell J, Fenwick K, Kozarewa I, Orr NJ, Lord CJ, Ashworth AA, and McCance DJ (2014). Genome- wide characterization reveals complex interplay between TP53 and TP63 in response to genotoxic stress. Nucleic Acids Res. 42, 6270–6285. [PubMed: 24823795]

Mejlvang J, Kriajevska M, Vandewalle C, Chernova T, Sayan AE, Berx G, Mellon JK, and Tulchinsky E (2007). Direct repression of cyclin D1 by SIP1 attenuates cell cycle progression in cells undergoing an epithelial mesenchymal transition. Mol. Biol. Cell 18, 4615–4624. [PubMed: 17855508]

Mermel CH, Schumacher SE, Hill B, Meyerson ML, Beroukhim R, and Getz G (2011). GISTIC2.0facilitates sensitive and confident localization ofthe targets of focal somatic copy-number alteration in human cancers. Genome Biol. 12, R41. [PubMed: 21527027]

Mills AA, Zheng B, Wang XJ, Vogel H, Roop DR, and Bradley A (1999). p63 is a p53 homologue required for limb and epidermal morphogenesis. Nature 398, 708–713. [PubMed: 10227293]

Moon S, Han D, Kim Y, Jin J, Ho WK, and Kim Y (2014). Interactome analysisofAMP-activated proteinkinase(AMPK)-a1 and-p1 in INS-1 pancreatic beta-cells by affinity purification-mass spectrometry. Sci. Rep. 4, 4376. [PubMed: 24625528]

Mrazek J, and Xie S (2006). Pattern locator: a new tool for finding local sequence patterns in genomic DNA sequences. Bioinformatics 22, 3099–3100. [PubMed: 17095514]

Mundt HM, Stremmel W, Melino G, Krammer PH, Schilling T, and Müller M (2010). Dominant negative (DeltaN) p63alpha induces drug resistance in hepatocellular carcinoma by interference with apoptosis signaling pathways. Biochem. Biophys. Res. Commun. 396, 335–341. [PubMed: 20403333]

Nagao M, Kaziro Y, and Itoh H (1999). The Src family tyrosine kinase is involved in Rho-dependent activation ofc-Jun N-terminal kinase by Galpha12. Oncogene 18, 4425–4434. [PubMed: 10442633]

Neilsen PM, Noll JE, Suetani RJ, Schulz RB, Al-Ejeh F, Evdokiou A, Lane DP, and Callen DF (2011). Mutant p53 uses p63 as a molecularchap- erone to alter gene expression and induce a pro-invasive secretome. Oncotar- get 2, 1203–1217.

Nekulova M, Holcakova J, Coates P, and Vojtesek B (2011). The role of p63 in cancer, stem cells and cancer stem cells. Cell. Mol. Biol. Lett. 16, 296–327. [PubMed: 21442444]

Ottley E, and Gold E (2014). microRNA and non-canonical TGF-β signalling: implications for prostate cancer therapy. Crit. Rev. Oncol. Hematol. 92, 49–60. [PubMed: 24985060]

Palomero T, Couronné L, Khiabanian H, Kim MY, Ambesi-Impiombato A, Perez-Garcia A, Carpenter Z, Abate F, Allegretta M, Haydu JE, et al. (2014). Recurrent mutations in epigenetic regulators, RHOA and FYN kinase in peripheral T cell lymphomas. Nat. Genet. 46, 166–170. [PubMed: 24413734]

Perez CA, Ott J, Mays DJ, and Pietenpol JA (2007). p63 consensus DNA-binding site: identification, analysis and application into a p63MH algorithm. Oncogene 26, 7363–7370. [PubMed: 17563751]

Ramsey MR, He L, Forster N, Ory B, and Ellisen LW (2011). Physical association of HDAC1 and HDAC2 with p63 mediates transcriptional repression and tumor maintenance in squamous cell carcinoma. Cancer Res. 71, 4373–4379. [PubMed: 21527555]

Ramsey MR, Wilson C, Ory B, Rothenberg SM, Faquin W, Mills AA, and Ellisen LW (2013). FGFR2 signaling underlies p63 oncogenic function in squamous cell carcinoma. J. Clin. Invest. 123, 3525–3538. [PubMed: 23867503]

Reuther GW, Lambert QT, Booden MA, Wennerberg K, Becknell B, Marcucci G, Sondek J, Caligiuri MA, and Der CJ (2001). Leukemia-associated Rho guanine nucleotide exchange factor, a Dbl family protein found mutated in leukemia, causes transformation by activation of RhoA. J. Biol. Chem. 276, 27145–27151. [PubMed: 11373293]

Ridley A (2013). GTPaseswitch: Rasthen Rhoand Rac. Nat. Cell Biol. 15,337. [PubMed: 23548925]

Rocco JW, Leong CO, Kuperwasser N, DeYoung MP, and Ellisen LW (2006). p63 mediates survival in squamous cell carcinoma by suppression of p73-dependent apoptosis. Cancer Cell 9, 45–56. [PubMed: 16413471]

Rodrigues P, Macaya I, Bazzocco S, Mazzolini R, Andretta E, Dopeso G, Mateo-Lozano S, Bilic J, Carton-Garcia F, Nieto R, et al. (2014). RHOA inactivation enhances Wnt signalling and promotes colorectal cancer. Nat. Commun. 5, 5458. [PubMed: 25413277]

Sakata-Yanagimoto M, Enami T, Yoshida K, Shiraishi Y, Ishii R, Miyake Y, Muto H, Tsuyama N, Sato-Otsubo A, Okuno Y, et al. (2014). Somatic RHOA mutation in angioimmunoblastic T cell lymphoma. Nat. Genet. 46, 171–175. [PubMed: 24413737]

Saladi SV, Ross K, Karaayvaz M, Tata PR, Mou H, Rajagopal J, Ram- aswamy S, and Ellisen LW (2017). ACTL6A Is Co-Amplified with p63 in SquamousCell Carcinomato DriveYAPActivation, Regenerative Proliferation, and Poor Prognosis. Cancer Cell 31, 35–49. [PubMed: 28041841]

Sánchez NS, and Barnett JV (2012). TGFβ and BMP-2 regulate epicardial cell invasion via TGFpR3 activation of the Par6/Smurf1/RhoA pathway. Cell. Signal. 24, 539–548. [PubMed: 22033038]

Schneider CA, Rasband WS, and Eliceiri KW (2012). NIH Image to ImageJ: 25 years of image analysis. Nat. Methods 9, 671–675. [PubMed: 22930834]

Senoo M, Pinto F, Crum CP, and McKeon F (2007). p63 Is essential for the proliferative potential of stem cells in stratified epithelia. Cell 129, 523–536. [PubMed: 17482546]

Shalem O, Sanjana NE, Hartenian E, Shi X, Scott DA, Mikkelson T, Heckl D, Ebert BL, Root DE, Doench JG, and Zhang F (2014). Genome-scale CRISPR-Cas9 knockout screening in human cells. Science 343, 84–87. [PubMed: 24336571]

Subramanian A, Tamayo P, Mootha VK, Mukherjee S, Ebert BL, Gillette MA, Paulovich A, Pomeroy SL, Golub TR, Lander ES, and Mesirov JP (2005). Gene set enrichment analysis: a knowledge-based approach for interpreting genome-wide expression profiles. Proc. Natl. Acad. Sci. USA 102, 15545–15550. [PubMed: 16199517]

Sullivan KD, Lewis HC, Hill AA, Pandey A, Jackson LP, Cabral JM, Smith KP, Liggett LA, Gomez EB, Galbraith MD, et al. (2016). Trisomy 21 consistently activates the interferon response. eLife 5, e16220. [PubMed: 27472900]

Vega S, Morales AV, Ocana OH, Valdes F, Fabregat I, and Nieto MA (2004). Snail blocks the cell cycle and confers resistance to cell death. Genes Dev. 18, 1131–1143. [PubMed: 15155580]

Watanabe N, Madaule P, Reid T, Ishizaki T, Watanabe G, Kakizuka A, Saito Y, Nakao K, Jockusch BM, and Narumiya S (1997). p140mDia, a mammalian homolog of Drosophila diaphanous, is a target protein for Rho small GTPase and is a ligand for profilin. EMBO J. 16, 3044–3056. [PubMed: 9214622]

Westfall MD, Mays DJ, Sniezek JC, and Pietenpol JA (2003). The Delta Np63 alpha phosphoprotein bindsthe p21 and 14–3-3 sigma promoters in vivo and has transcriptional repressor activity that is reduced by Hay-Wells syndrome-derived mutations. Mol. Cell. Biol. 23, 2264–2276. [PubMed: 12640112]

Yang A, Kaghad M, Wang Y, Gillett E, Fleming MD, Dötsch V, Andrews NC, Caput D, and McKeon F (1998). p63, a p53 homolog at 3q27–29, encodes multiple products with transactivating, death-inducing, and dominant-negative activities. Mol. Cell 2, 305–316. [PubMed: 9774969]

Yoo HY, Sung MK, Lee SH, Kim S, Lee H, Park S, Kim SC, Lee B, Rho K, Lee JE, et al. (2014). A recurrent inactivating mutation in RHOA GTPase in angioimmunoblastic T cell lymphoma. Nat. Genet. 46, 371–375. [PubMed: 24584070]

Zaborowska J, Egloff S, and Murphy S (2016). The pol II CTD: newtwists in the tail. Nat. Struct. Mol. Biol. 23, 771–777. [PubMed: 27605205]

Zhang B, and Zheng Y (1998). Regulation of RhoA GTP hydrolysis by the GTPase-activating proteins p190, p50RhoGAP, Bcr, and 3BP-1. Biochemistry 37, 5249–5257. [PubMed: 9548756]

Highlights

- CRISPR screen identifies RHOA as mediator of proliferation arrest upon ΔNp63α depletion
- ΔNp63α suppresses RHOA activity and TGFB2 expression
- TGFB2 is sufficient to activate RHOA and impair SCC cell proliferation
- Neutralization of TGFB2 restores SCC cell proliferation during ΔNp63α depletion

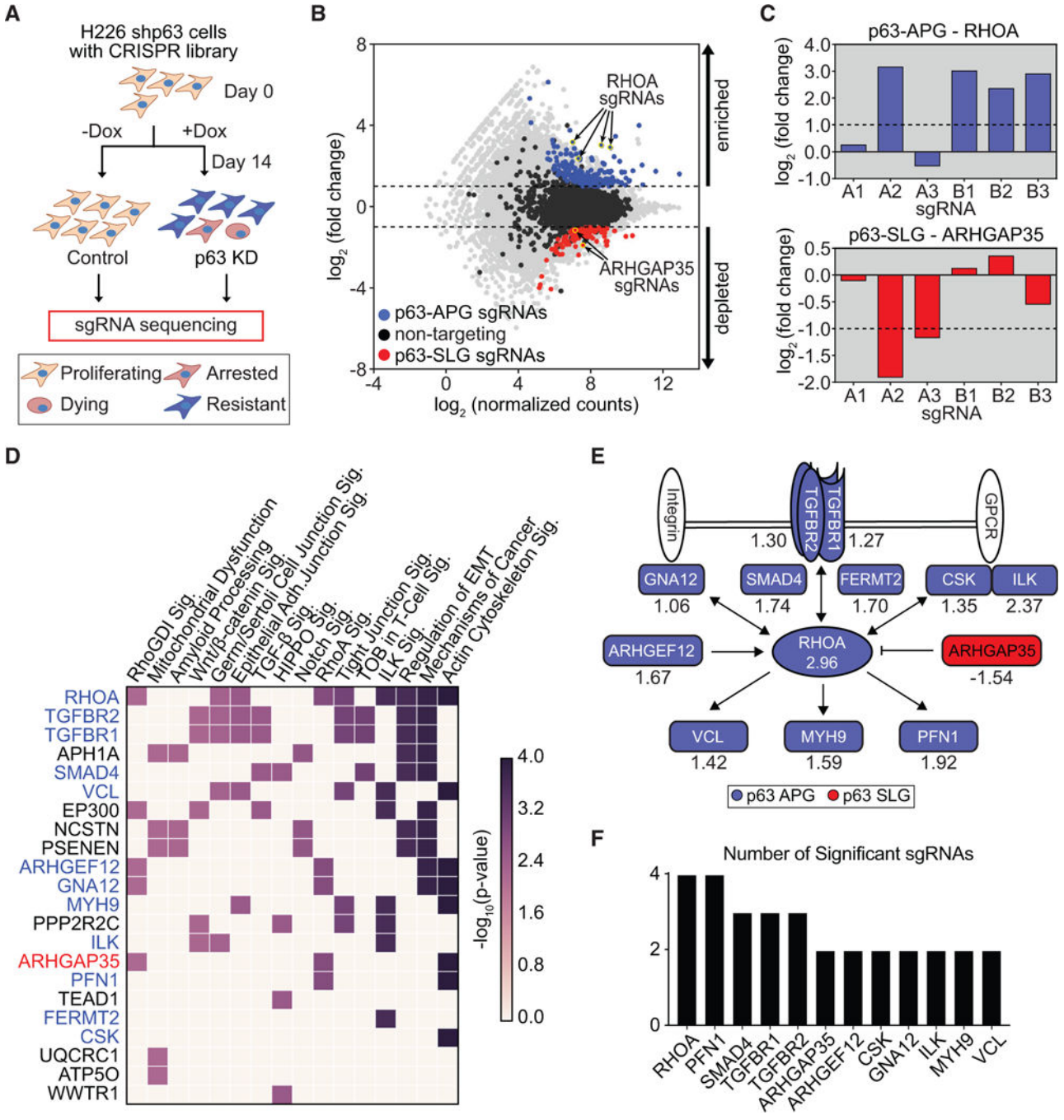

Figure 1. A CRISPR Screen Identifies RHOA Signaling as a Negative Regulator of ΔNp63α-Driven Cell Proliferation

(A) Outline of the CRISPR screening strategy in H226 cells using the Human GeCKOv2 libraries. (B) MA plotfor individual sgRNAs detected at the conclusion ofthe screen. The 1,000 non-targeting control sgRNAs are highlighted in black, whereas significant sgRNAs (adjusted $p < 0.05$, fold change ≥ 2) for genes where at least two sgRNAs met these thresholds are highlighted in blue and red forenriched and depleted sgRNAs, respectively. (C) Fold change values for all six sgRNAs; for example, p63-APG (*RHOA*) and p63-SLG (*ARHGAP35*) candidates. (D) Plot showing membership of individual p63-APG and p63-

SLG candidates across the top canonical pathways ($p < 0.005$) enriched among the 141 high-confidence screen hits, as revealed by Ingenuity Pathway Analysis. Genes within each pathway are color-coded by — $\log_{10}$-transformed pathway enrichment p values. (E) Schematic showing known relationshipsamong p63-APG (blue) and p63-SLG (red) candidates related to RHOAsignaling (see main textfor references). Listed below each candidate is the $\log_2$-transformed median fold change for significant sgRNAs targeting that gene. (F) Number of significant sgRNAs (adjusted $p < 0.05$, fold change ≥ 2) for p63-APG and p63-SLG candidates included in (E). See also Figure S1 and Table S1.

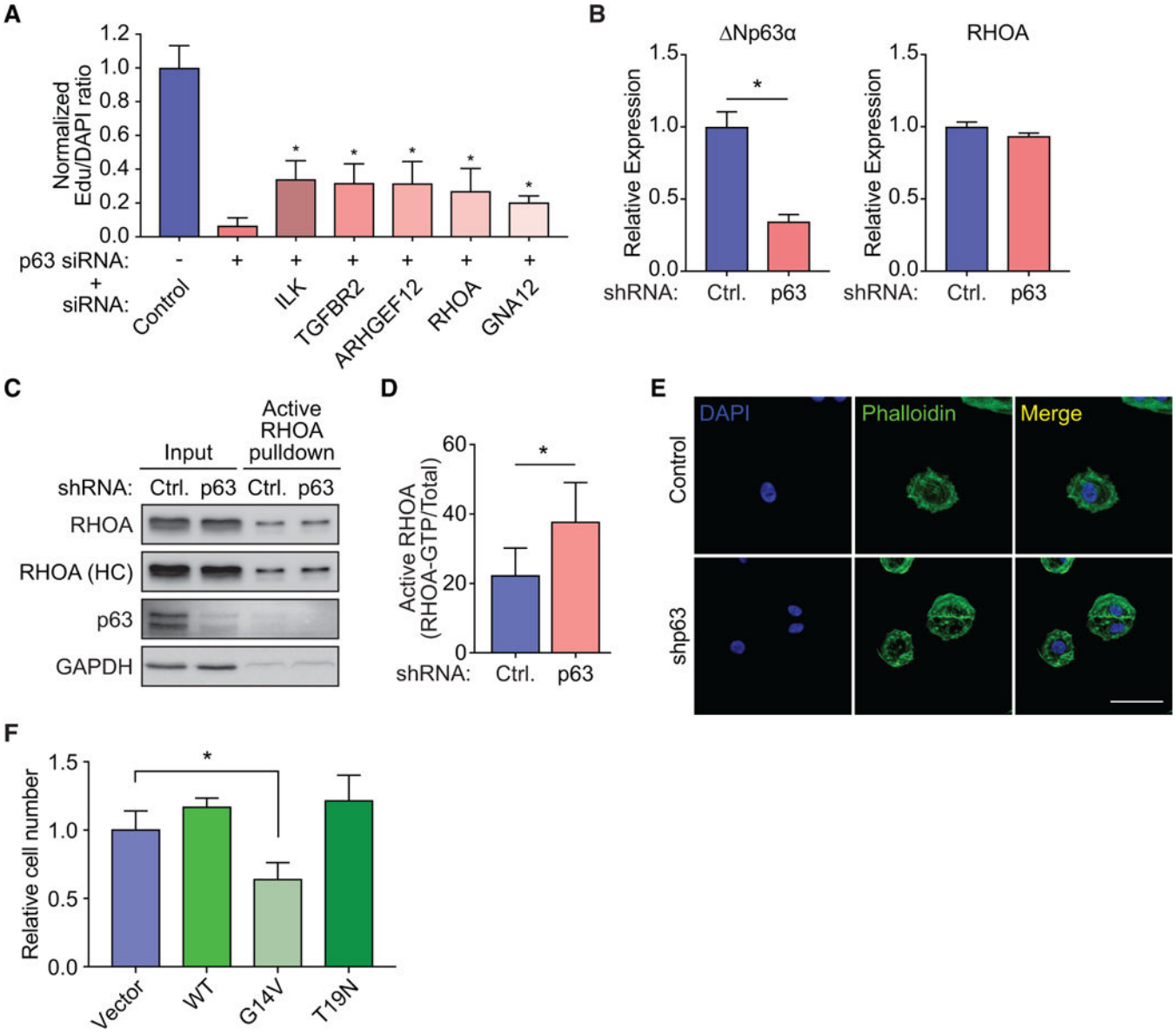

Figure 2. RHOA Signaling Blocks Cell Proliferation upon Depletion of ΔNp63α

(A) Relative EdU signal forH226 cells treated with the indicated siRNA combinations.Values were normalized to the DAPI signal and are expressed relative to cells treated with control siRNAonly. Data are represented as mean ± SEM from three independent replicates. Asterisks indicate significant differences in comparison to p63 siRNA alone (unpaired t test, *p < 0.05). (B) Relative mRNA expression for ΔNp63α and RHOA in H226 cells expressing control or p63-targeting shRNAs. Values were normalized to 18S ribosomal RNA and are expressed relative to the mean of control shRNA-expressing cells. Data are represented as mean ± SEM from three independent replicates. Asterisk indicates significant difference (unpaired t test, *p < 0.05). (C) Western blot showing levels of RHOA, p63, and GAPDH in cell lysates (input) and in a pull-down of active Rho proteinsfrom H226 cells expressing control or p63-targeting shRNAs. The blot labeled RHOA (HC) has been adjusted for higher contrast in the pull-down lanes. (D) Quantification

of active RHOA levels from the active RHOA pull-down assay. Values were normalized to total RHOA levels in input lysates. Data are represented as mean ± SEM from four independent replicates. The asterisk indicates significant difference (unpaired t test, *p < 0.05). (E) Representative images of H226 control and shp63 cells stained with DAPI and phalloidin. Scale bar, 25 μm. (F) Relative cell numbersfor H226 cells 72 hraftertransfection with expression constructsforwild-type (WT), constitutivelyactive(G14V), and dominant-negative (T19N) RHOA. Values are expressed relative to cells transfected with vector alone. Data are represented as mean ± SEM from three independent replicates. Asterisk indicates significant difference (unpaired t test, *p < 0.05). See also Figure S2.

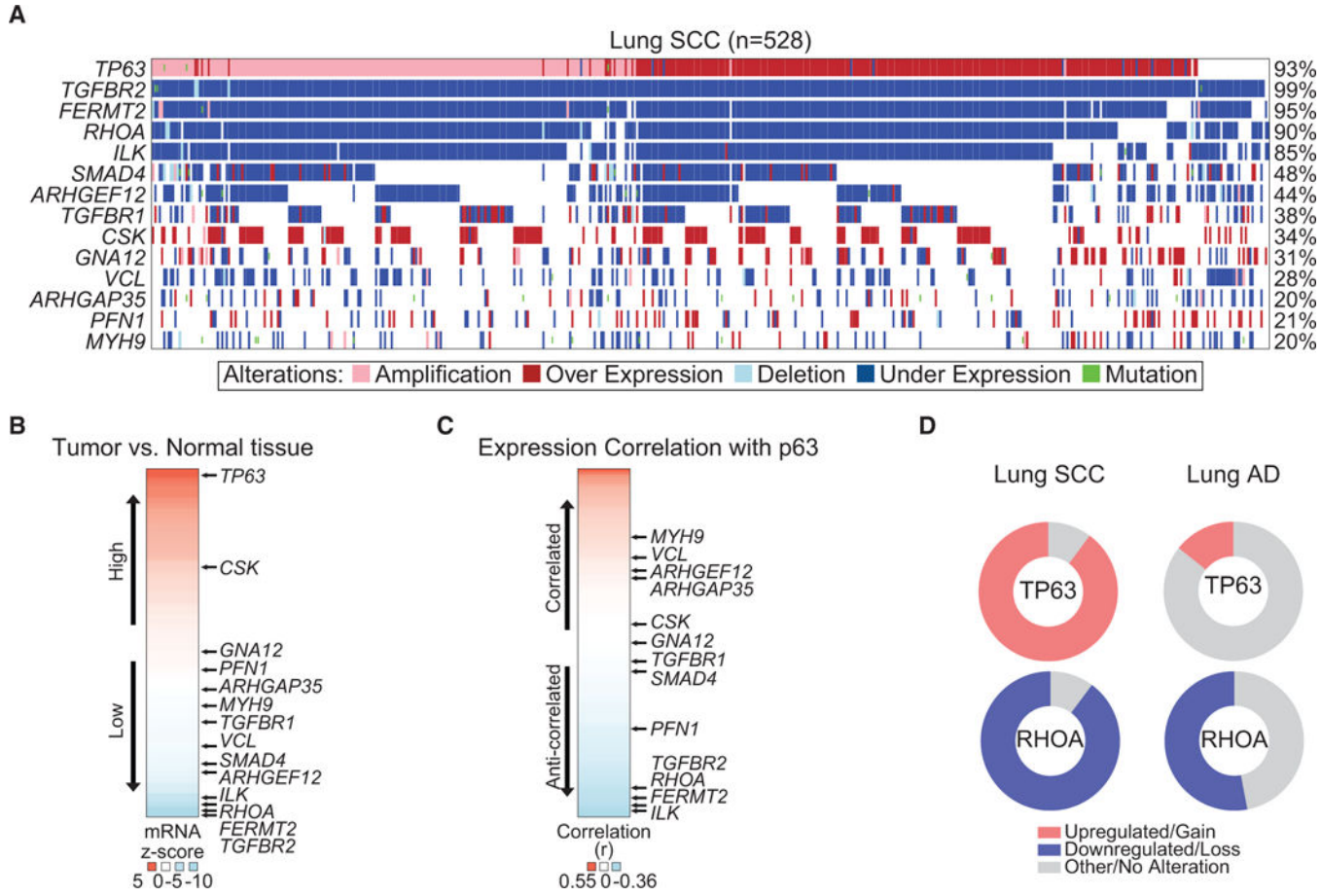

Figure 3. Components of the RHOA Signaling Network Are Commonly Repressed in Lung SCCTumors

(A) Oncoprint of TP63 and 13 genes associated with the TGF-β and RHOA signaling pathways identified in the CRISPR screen. (B) Heat map of expression levels (tumor versus normal tissue) for the 141 genesthat scored as significant in the CRISPR screen. Genes are ranked in descending order based upon *Z* scores calculated from RSEM (RNA-seq by expectation maximization) values relative to healthy tissue. Genes in the TGF-β and RHOA signaling pathways are indicated with arrows. (C) Heatmap of pairwise Pearson correlations to TP63 expression (RSEM V2) for each of the 141 screen hits. (D) Donut plotswith combined copy numbervariation and expression data showing the proportion of lung SCC and lung adenocarcinoma (AD) samples with gain or loss of TP63 and RHOA.

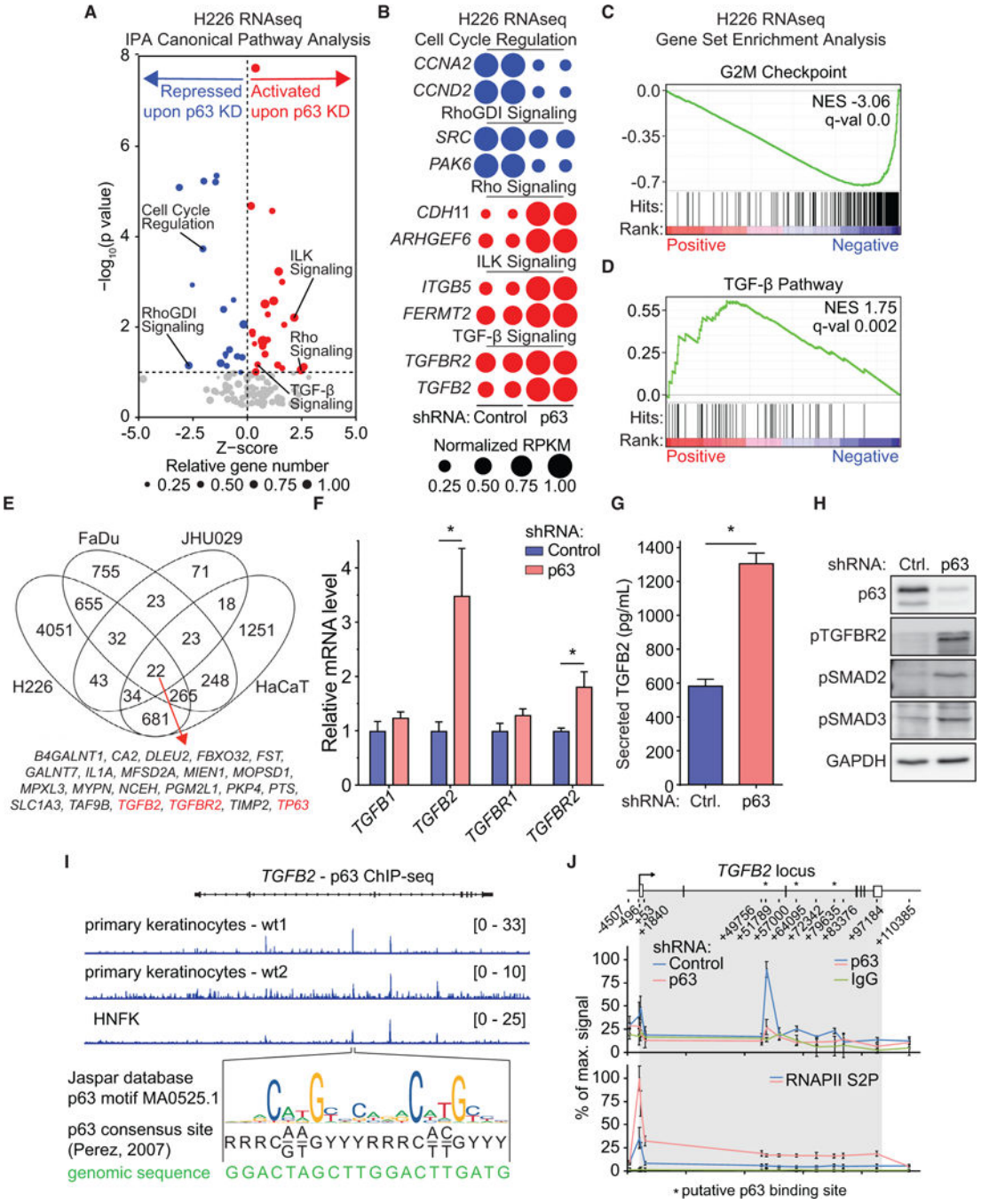

Figure 4. ΔNp63α Represses Transcription of TGFB2, an Upstream Activator of RHOA

(A) Volcano plot of activation Zscores against p values for Ingenuity Canonical Pathways Analysis of genes differentially expressed between shControl and shp63 H226 cells after 6 days of doxycycline treatment to induce shRNA expression. The circled areas are proportional to the number of genes with significant expression changes (adjusted $p < 0.1$). (B) Bubble plots showing relative expression of selected genes from enriched pathways in shControl and shp63 H226 cells. Circle areas are proportional to RPKM (reads per kilobase per million mapped reads) levels), normalized per gene. (C and D) Gene set enrichment

analysis (GSEA) plots for the G2M (C) and TGF-β pathway (D) hallmark gene sets, with black bars indicating where gene set members fall among all genes when ranked by log2-transformed ratio (shp63/shControl). (E) Venn diagram of genes differentially expressed upon p63 depletion in H226, FaDu, JHU029, and HaCaT cells. (F) Relative mRNA expression for *TGFB1, TGFB2, TGFBR1*, and *TGFBR2* in shControl and shp63 H226 cells as defined by qRT-PCR. Values were normalized to 18S ribosomal RNA and are expressed relative to the mean of shControl cells. Data are represented as mean ± SEM from three independent replicates. Asterisks indicate significant differences (unpaired t test, $*p < 0.05$). (G) Levels of TGFB2 in culture supernatants of shControl and shp63 H226 cells, as measured by ELISA. Data are represented as mean ± SEM from three independent replicates. Asterisk indicates significant difference (unpaired t test, $*p < 0.05$). (H) Western blot showing levels of p63, phospho-TGFBR2, phospho-SMAD2, phospho-SMAD3, and GAPDH in shControl and shp63 H226 cells. (I) p63 ChIP-seq tracks from primary keratinocytes (Kouwenhoven, 2010) and human normal foreskin (HNFK) cells (McDade et al., 2014). Shown at the bottom are the Jaspar database p63 position-weight matrix (Mathelier et al., 2016), p63 consensus site (Perez et al., 2007), and genomic sequence of the indicated loci. (J) ChIP analysis of p63 and serine-2-phosphorylated Pol II (Pol II S2P) at the *TGFB2* locus in shControl and shp63 H226 cells. To represent profiles across the locus, values are plotted as the percentage of maximum signal for each epitope. Data are represented as mean ± SEM from three independent replicates. The gray area indicates the transcribed region. Black tick marks indicate the position of each amplicon. See also Figure S3 and Table S2.

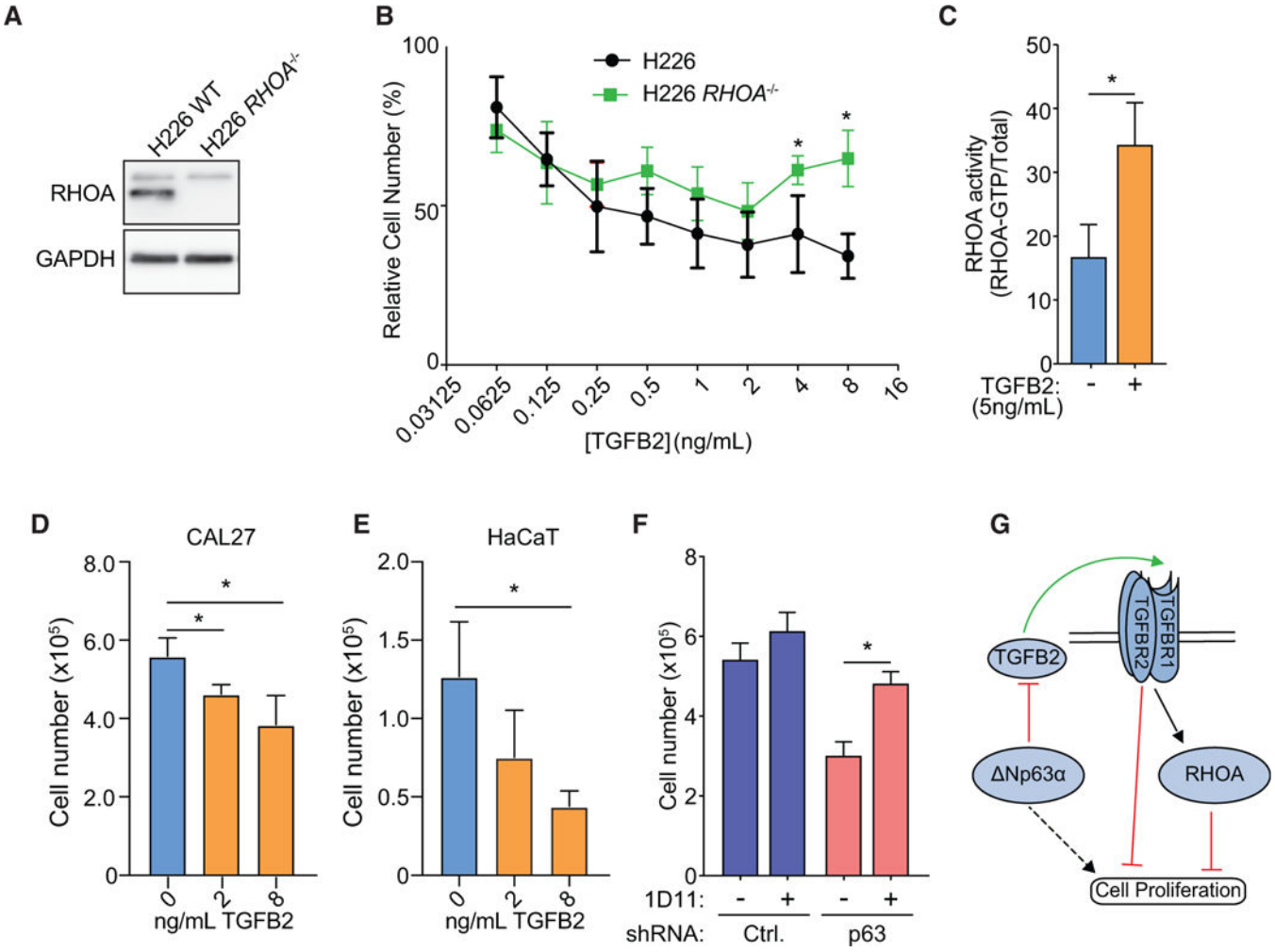

Figure 5. Elevated TGFB2 Contributes to Cell Cycle Arrest upon Depletion of ΔNp63α

(A) Western blot showing levels of RHOA and GAPDH in WT and RHOA$^{-/-}$ H226 cells. (B) Relative number of WT and RHOA$^{-/-}$ H226 in response to increasing doses of recombinant TGFB2. (C) Quantification of active RHOA levels in pull-down from lysates from H226 cells with or without recombinant TGFB2. Values were normalized to total RHOA levels in input lysates. Data are represented as mean ± SEM from three independent replicates. The asterisk indicates significant difference (unpaired t test, *p < 0.05). (D) Cell counts for CAL27 cells after treatment with increasing doses of recombinant TGFB2 for 72 hr. (E) Cell counts for HaCaT cells after treatment with increasing doses of recombinant TGFB2 for 72 hr. (F) Cell countsfor control and shp63 H226 cellsafter96 hrtreatment with theTGF-β-neutralizing antibody 1D11. Dataare represented as mean ± SEM from three independent replicates. The asterisk indicates significant difference (unpaired t test, *p < 0.05). (G) Model summarizing the results reported here, whereby the TGFB2 to RHOA signaling pathway is required to enforce proliferation arrest upon ΔNp63α depletion. For data in (B)-(F), data are represented as mean ± SEM from three independent replicas. Asterisk indicates significant difference (unpaired t test, *p < 0.05).